Barrier-limited surface diffusion in atom lithography

E. te Sligte,[a] K. M. R. van der Stam, B. Smeets, P. van der Straten, R. E. Scholten,[b] H. C. W. Beijerinck, and K. A. H. van Leeuwen[c]
Department of Applied Physics, Eindhoven University of Technology, P.O. Box 513, 5600 MB Eindhoven, The Netherlands

(Received 18 July 2003; accepted 10 November 2003)

Thermally activated surface diffusion has a strong influence on structure widths in atom lithography. We investigate the effects of two barriers to thermally activated atomic diffusion on atom lithography: a thermally activated Ehrlich–Schwoebel (ES) barrier, and pollution from the residual gas in the vacuum system. We performed kinetic Monte Carlo simulations using a one-dimensional surface grid. We find that the ES barrier fails to explain the lack of temperature dependence observed experimentally [W. R. Anderson *et al.*, Phys. Rev. A **59**, 2476 (1999)]. The dependencies of the structure width on temperature, vacuum conditions, and beam characteristics can be explained using the pollutant adatom hypothesis. Only the variation of structure width with deposition duration was not entirely reproduced by this model. We attribute this to the one-dimensional nature of our simulations. These results demonstrate that barrier-limited diffusion can play an important role in atom lithography, and that pollutant adatoms are a likely candidate barrier. © *2004 American Institute of Physics.* [DOI: 10.1063/1.1638613]

I. INTRODUCTION

One of the many applications of the optical dipole force[1] is atom lithography.[2] In this technique, a laser light field induces an electrical dipole moment in atoms passing through it. This electrical dipole experiences a force from the intensity gradient of the light field. Using a plane standing wave, as shown in Fig. 1, the light field will function as an array of lenses, focusing the atoms to the nodes or antinodes for light frequencies above or below the atomic resonance. By placing a substrate in the focal plane, the atoms are deposited onto this substrate with a spatially modulated flux distribution with half-wavelength period. The resulting structures can be investigated *ex situ* by techniques such as atomic force microscopy (AFM). The main advantages of this lithography technique are its compatibility with molecular beam epitaxy (MBE) (Ref. 3) and its considerable parallelism.[4]

This kind of experiment has been performed using Na,[5] Cr,[6] and Al (Ref. 7) atoms, and our group is pursuing it for Fe atoms.[8] In the case of Cr, an extensive study on structure widths was done by Anderson *et al.*[9] They found that the structures deposited were always 20–30 nm wider than the incoming atomic beam flux distribution. Due to the confidence and thoroughness with which this atomic beam flux distribution can be calculated, they concluded that the broadening of the nanostructures must be caused by a diffusion process on the substrate. However, the broadening proved oddly independent of substrate temperature. In Na deposition experiments by Behringer *et al.*,[10] details of the sample preparation method were shown to be of crucial importance to the diffusion effects. Samples heat cleaned in a very well-baked-out ultra-high-vacuum (UHV) chamber proved to be so susceptible to surface diffusion that there were no visible structures at the end of the deposition. Samples prepared in an unbaked vacuum chamber showed no signs of surface diffusion. Behringer *et al.*[10] attribute this effect to residual hydrocarbons on the sample surface that limit surface diffusion and act as nucleation sites.

Jurdík *et al.*[11] attempt to explain the broadening of the Cr nanostructures using thermally activated surface diffusion as a mechanism. They explore various atomistic models, and find that the resulting structures show a very strong dependence on substrate temperature and on the diffusion parameters. This result prompted Bradley *et al.*[12] to investigate the hypothesis that the surface diffusion was caused by the energy released when the atoms hit the surface, a process dubbed impact cascade diffusion (ICD). However, this theory does not explain the immense dependence on sample preparation conditions found by Behringer *et al.*[10] As Jurdík *et al.* point out, their thermal surface diffusion model does not take into account the effects of pollution.

In this article, we consider two alternative explanations for this diffusion effect. One possible explanation is that pollutants such as hydrocarbons, oxygen, etc., act as a limiting factor on the surface diffusion effects observed in atom lithography experiments. A clear indication of this can be found in the extreme dependence on vacuum conditions that Behringer *et al.*[10] find. The other effect under consideration is the possibility that surface diffusion might be limited by an increased hopping activation energy at terrace boundaries. This effect is well known in surface physics and is called the Ehrlich–Schwoebel (ES) barrier.[13]

The remainder of this article will be dedicated to our numerical investigation of structure broadening in atom lithography. We begin by describing the model we use in Sec. II, and will continue by assigning values to most of its free

[a]Electronic mail: e.t.sligte@tue.nl
[b]Also at: School of Physics, University of Melbourne, Australia.
[c]URL: http://www.phys.tue.nl/aow

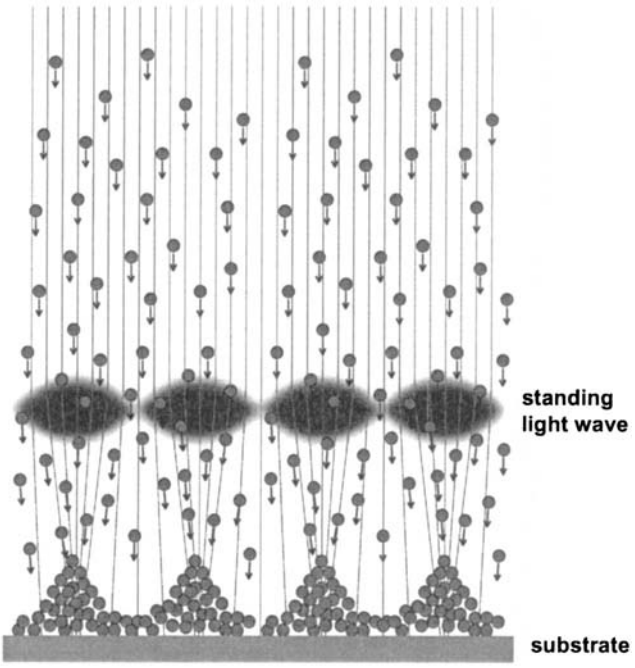

FIG. 1. Direct-write atom lithography schematic. Atoms are deflected and focused by the laser standing wave and follow the trajectories indicated. They are deposited onto the substrate, where a periodic structure is generated.

parameters in Sec. III. Then, we first display the results of the pollution hypothesis in Sec. IV, followed by those of the ES-barrier scenario in Sec. V. We compare both hypotheses in Sec. VI.

II. NUMERICAL MODEL

We model atom lithography as a process in which atoms impinge perpendicularly on a surface. The atoms focused by the light field have a lateral distribution, which we assume to be Lorentzian in shape. We assume that some of the atoms will not be focused by the standing light wave, mainly because of imperfections in the atom beam. They are described as a homogeneous background flux. The surface is described as a one-dimensional linear grid of sites. We limit our model to one dimension to limit the complexity of the code and reduce calculation times. The grid spacing is assumed to be equal to the lattice constant for Cr. We set the grid size to the period of the incoming atom flux distribution, 212 nm for Cr. This corresponds to 739 sites for a lattice constant of 0.287 nm. Initially, the surface is flat and nonreactive. We apply periodic boundary conditions to the surface.

Once on the surface, the atoms are able to hop from site to site. We assume all hopping processes are likely equally, provided that the atoms can move without reducing their number of nearest neighbors. Processes that require reduction of the number of nearest neighbors are not allowed. If hopping in both directions is allowed, hopping proceeds with 50% likelihood in either direction. If only one hopping direction is available, there is a 50% chance that the atom remains stationary, and a 50% chance that it will hop in the available direction. If both hopping directions are blocked, the atom remains stationary. This model implies that a cluster of two atoms is a stable island, and that diffusion across planes at a slope of 45° occurs as quickly as on horizontal planes. The frequency of hopping steps is assumed constant, and given by the Arrhenius relation:

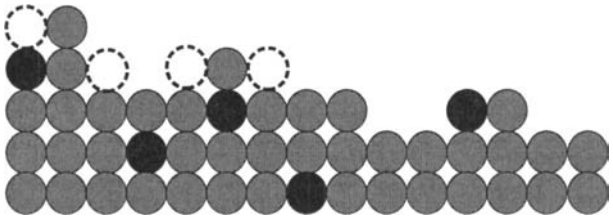

FIG. 2. Artifacts in our diffusion model. Gray circles: deposited atoms. Dark circles: pollutant species. Dashed circles: sites to which a deposited atom may hop. Atoms move freely to sites that have no fewer neighbors than their present site, but not at all to sites that have fewer nearest neighbors. Pollutant species cannot diffuse at all and act as diffusion inhibitors.

$$R_{\mathrm{hop}} = R_0 e^{-E_d/k_B T}, \tag{1}$$

where R_0 is the lattice frequency of the material, which we assume to be $10^{12}\,\mathrm{s}^{-1}$; k_B is Boltzmann's constant; and T is temperature (in degrees K). We perform all simulations at $T = 300\,\mathrm{K}$ unless otherwise stated.

We incorporate a possible ES barrier by assigning a greater activation energy $E_d + E_{\mathrm{ES}}$, and thus a reduced hopping chance to atoms stepping down from a terrace. Atoms cannot step up onto a terrace, as doing so would reduce their number of nearest neighbors. The ES hopping rate is given by

$$R_{\mathrm{ES}} = R_0 \mathrm{e}^{-(E_{ES}+E_d)/k_B T} = R_{\mathrm{hop}} \mathrm{e}^{-E_{ES}/k_B T}. \tag{2}$$

The pollution is represented as a homogenous flux of pollutant species from the residual gas in the vacuum system. We assume that these pollutants will stick on the site where they hit the substrate if and only if they land on top of a chemically active (nonpollutant, nonsubstrate) atom. There, they occupy exactly one atomic grid position each. They cannot diffuse at all in our model.

Our diffusion model incorporates two distinct time scales. Usually, the fastest of these by far is the regularized hopping time, which is $\tau_{\mathrm{hop}} \sim 10^{-7}\,\mathrm{s}$ at room temperature, but extremely sensitive to changes in temperature and hopping activation energy. The time between atom arrivals on the whole grid τ_{dep} is, typically, in the tens of milliseconds. For low temperatures, the two are not necessarily orders of magnitude apart. We compensate for this by running an internal clock with clock time 0.1 times the shortest time scale if the two time scales are less than an order of magnitude apart. If $\tau_{\mathrm{hop}} \leqslant 0.1\tau_{\mathrm{dep}}$, the hopping time is taken as clock time. We then round the longer time scale to an integer number of clock ticks.

Figure 2 displays some of the possibilities and artifacts in our diffusion model. Left, an atom on a step edge can step down or move away from the edge. If $E_{\mathrm{ES}} = 0$, both processes are equally likely. In the case of ES-barrier simulations, the atom has 50% chance to move away from the step, and a small chance to cross it. If neither happens, the atom does nothing during this diffusion step. In the center, atomic motion over pollutants embedded in the surface is unim-

peded. Right, an atom that encounters a pollutant species is fixed, as moving would require reduction of its number of nearest neighbors. Also, an atom that is part of a step edge is immobile, and will never be able to detach itself from the step edge. In ES-barrier-based simulations, pollutants are absent.

The model presented above is similar to the diffusion model Jurdík *et al.* judged the most realistic.[11] However, we do not allow for diffusion processes that reduce the number of nearest neighbors. This means that, contrary to the model used in Ref. 11, the diffusion process is self-terminating, and the resulting structures will be permanent. For the case of Cr, the structures do indeed remain intact for months or even years after deposition.

The key assumption in the pollutant model is that pollutant species exhibit no surface diffusion whatsoever. This extreme assumption is appropriate if the pollutant hopping rate is much smaller than that of the lithographically deposited atoms. For oxygen adatoms, there are several experiments that indicate near-total surface immobility of adatoms.[14,15]

III. SIMULATION PARAMETERS

We will now proceed to choose our parameters, being the atomic beam flux density profile, the pollutant flux density, the deposition time, the hopping activation energy, and the ES-barrier energy.

The atomic beam flux density profile is assumed to be a Lorentz distribution on top of a homogeneous background, with a width equal to the values calculated by Anderson *et al*. We choose the contrast ratio (peak height to homogeneous background level) to be 3.5; our own simulations of focusing find that this is a reasonable value in many cases. From the experimental data given by Anderson *et al.*,[9] we deduce that the spatially averaged beam flux density was around 0.05 ML/s ($1\ \mathrm{ML}=1.21\times10^{19}\ \mathrm{m}^{-2}$). The deposition time is set at 5 min, as in the Anderson experiment. The incoming flux distribution full width at half maximum (FWHM) remains fixed at 20 nm when other parameters are varied.

The diffusion activation energy E_d is the only free parameter in Eq. (1), and its absolute value is unknown: the surface diffusion activation energy for Cr has never been investigated experimentally. Only one calculation of its value is known to the authors; Schindler[16] calculates a value of 0.22 eV for Cr[110]. In the same work, he also finds values of 0.28 eV for Fe[110] and 0.47 eV for W[110]. Experimental values for these systems are 0.225 and 0.87 eV, respectively. For other crystal faces, the diffusion energies of Fe are consistently higher than those on the [110] face. We conclude that for the structures under consideration, which are most likely polycrystalline, the calculated value of 0.22 eV should be taken as a lower limit. We choose to perform the simulations using an effective hopping activation energy $E_d = 0.30$ eV.

We assume that the pollutant flux is constant and homogenous. We first make a rudimentary estimate of the amount of pollution needed to explain the experimental observations.

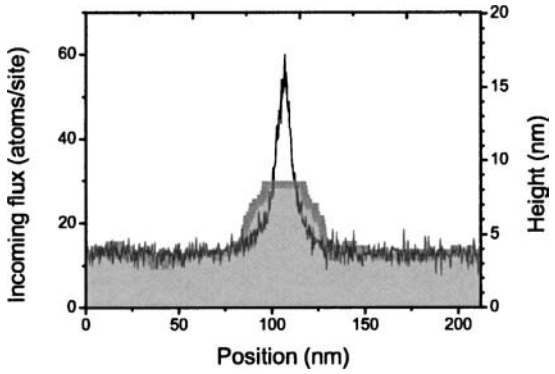

FIG. 3. Sample simulation results. Line: incoming flux distribution (10 nm FHWM); average of five runs. Filled curve: calculated diffusion-broadened structure (34 nm FWHM); single run.

The experimental structures are broadened by 20–30 nm with respect to the incoming atom flux distribution. Per structure flank, the broadening is 10–15 nm, or 35–50 sites. For a pollutant diffusion barrier, the distance to the nearest pollutant adatom should be on the order of the diffusion length. The corresponding amount of pollution is thus one in 35–50, or 2%–3%. In the absence of pollution, the diffusion length has no fundamental limit. Thus, the influence of a small amount of pollutants on the shape of the structures deposited could be immense.

The vacuum system was ion pumped to a pressure of around 10^{-8} mbar,[9] which corresponds to a molecular background flux of around 2.5×10^{-3} ML/s. The composition of the background gas is unknown. The literature indicates that the sticking chance of oxygen on Cr is close to unity.[17] For nitrogen, the sticking coefficient is similar.[18] Any water present can be assumed to stick as readily, and will therefore also contribute O or OH groups to the surface. As there are at most two atoms per molecule for these gases, we expect to find an effective chemically bonding pollutant flux of up to 5×10^{-3} ML/s. The estimate above results in a pollutant flux of 1×10^{-3}–1.5×10^{-3} ML/s, well within this range. The model value will be determined from the simulations.

The height of the ES barrier also has never been determined experimentally for Cr. However, for Fe/Fe[100], a value of 0.04 ± 0.01 eV was found,[19] and for Al/Al[111] 0.07 ± 0.01 eV was found.[20] For Al, values ranging from 0.04 eV to 0.83 eV have been calculated.[21] Comparing these values to the normal hopping energies, 0.454 eV for Fe[100] and 0.04 eV for Al[111], we find that the ES barrier is very small compared to the hopping energy for Fe, but at least comparable for Al. Given that we assume a hopping energy of 0.3 eV for Cr, we vary the ES barrier from 0 to 0.3 eV.

IV. POLLUTANT LIMITED SURFACE DIFFUSION

In this section, we investigate the results of the simulations under the assumption that $E_{\mathrm{ES}}=0$ eV. Thus, the only effect limiting surface diffusion is the presence of pollutant adatoms. Before investigating the dependencies of this model, we look at the structures it predicts. Figure 3 displays a sample incoming flux distribution and its resulting structure. To reduce statistical noise, we averaged five simulation

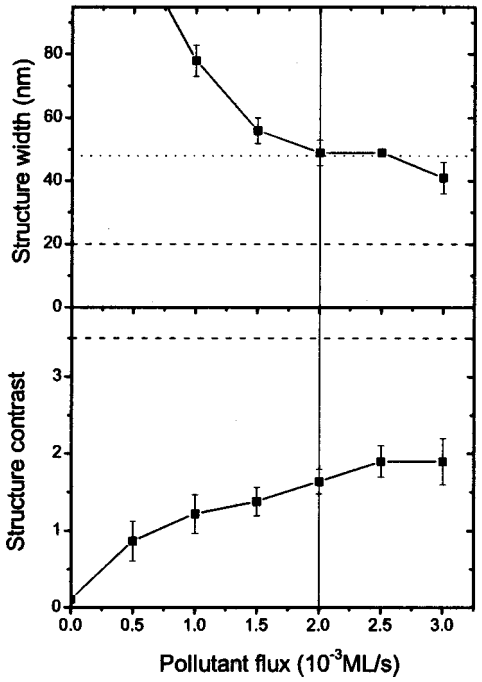

FIG. 4. Dependence of structure FWHM (top) and contrast ratio (bottom) on effective pollutant flux. Average of five runs; error bars indicate standard deviation. Dashed lines indicate model input values, dotted line indicates experimental value. As pollutants suppress diffusion, they preserve structure contrast and narrowness. Vertical line indicates model value.

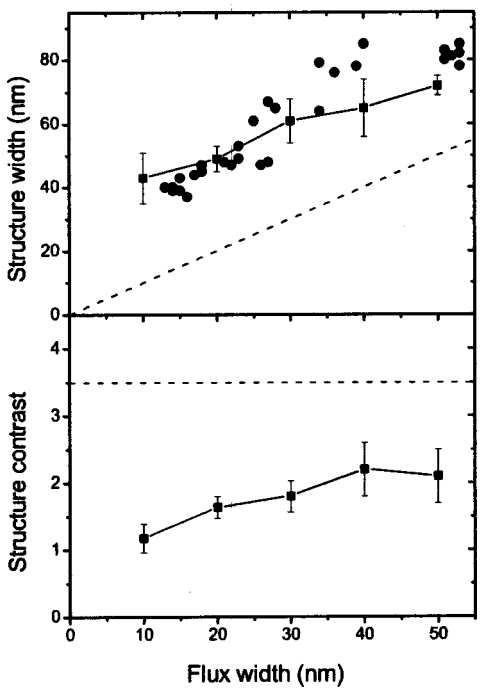

FIG. 5. Bottom: comparison between simulated structure widths and experimental data (circles) for varying flux distribution widths. Dashed line represents structure width equal to flux width. Top: simulated structure contrast for varying atom flux peak width. Dashed line indicates atomic flux contrast. Simulations are averages of five runs; error bars indicate standard deviations.

runs for the flux distribution. The incoming beam flux distribution with a width of 10 nm is transformed into a structure with a full width at half maximum of 34 nm. The height of the structure is also comparable to that found experimentally. As can be seen, the structure becomes broader and lower than that in the atom flux distribution, while the level of the background flux remains more or less the same. The top of the structure is a flat terrace; we attribute this to the fact that, in our model, atoms diffuse until they settle at a step edge. We conclude that diffusion primarily affects the shape of the structure. We find that the structure resembles the structures shown in experimental studies.[9]

We analyze the structures by two figures of merit; the width of the structure and its contrast. As the structures are not Lorentzian in shape, we determine their FWHM directly rather than from a curve fit. We define the contrast as the ratio of the height difference between the structure top and the background and the height difference between the background and substrate. We determine the background level by taking the average height of the leftmost 50 grid points. All structure widths and contrast ratios given from this point onwards are the averages of five simulation runs, and all error bars indicate standard deviations of these distributions.

Figure 4 shows the resulting structure FWHM and contrast as a function of effective pollutant flux. At low fluxes, diffusion clearly causes a lot of broadening. Also, the structure contrast is reduced strongly. These effects are very clearly suppressed by increasing pollution. The width of the structures found matches that found by Anderson *et al.*[9] for an effective pollutant flux of 2.0×10^{-3} ML/s. This is well within the range predicted in Sec. III, and close to the rough estimate in the introduction. We will use the value above throughout the remainder of this work. The pollution model has no further free parameters.

A. Atom flux

We can now proceed to compare the results of our model to the experimental investigations of Anderson *et al.*[9] That comparison is displayed at the bottom of Fig. 5. The data points have been taken directly from their paper, and have been plotted with the simulation results. We find very reasonable agreement between the experiments and our simulations, with the two being within two standard deviations of each other at all instances. Also shown is the incoming atom flux (dashed lines). The diffusive broadening appears to be constant. This confirms our model of atoms that can diffuse for a certain length until they encounter a pollutant atom. The contrast of these structures is shown in the top half of Fig. 5. As can be seen, it increases with increasing structure width. This supports our earlier conclusion that the background height is not enhanced by the diffusion processes, but that instead the peak area remains constant. The structure height then decreases as a result of the broadening.

Varying the atom flux contrast ratio, we found no effect on the resulting structure widths; however, we did find that a greater atom flux contrast gives a greater structure contrast, as shown in Fig. 6. This, too, favors the notion of the structure being smeared out by diffusion more or less independently from the background.

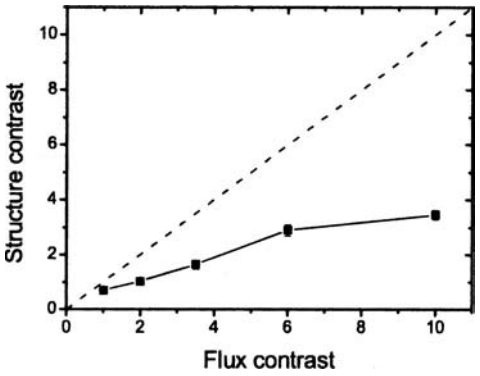

FIG. 6. Influence of flux contrast on structure contrast. Dashed line: structure contrast equal to flux contrast.

B. Temperature

One peculiar experimental result was the lack of temperature dependence. The temperature dependence of the results from our model is shown in Fig. 7. For a hopping activation energy of 0.3 eV, we find no temperature dependence above 250 K. Below this temperature, we find that the diffusion is limited by the low hopping rate rather than by pollution. At higher temperatures, when the diffusion length of an atom is determined by the distance to the nearest pollutant adatom or molecule, diffusion becomes temperature independent. Lowering the activation energy lowers the diffusion saturation temperature, as shown in Fig. 7. As the range of temperatures investigated by Anderson *et al.* runs from 200 to 350 K, we find that the effective diffusion barrier of Cr might be lower than we have assumed in this work. However, it is not a very critical parameter in our model. The other parameter from Eq. (1), R_0, has no influence on the simulation results if varied by a factor of 10. Temperature affects structure contrast as little as expected: there is no effect on contrast as long as there is no effect on structure width. Only at low temperatures or high diffusion energies does the contrast increase towards the value of the atomic beam flux contrast. This is a logical result in the absence of diffusion.

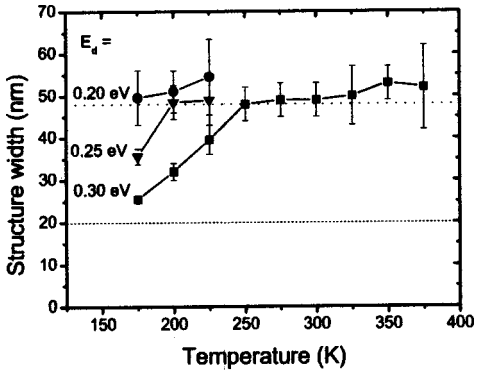

FIG. 7. Temperature dependence of the resulting structures. Dotted line indicates experimental value, dashed line indicates flux distribution. Squares: simulated widths, $E_d = 0.3$ eV. Triangles: simulated widths, $E_d = 0.25$ eV. Circles: simulated widths, $E_d = 0.2$ eV. Temperature has no influence over a wide range.

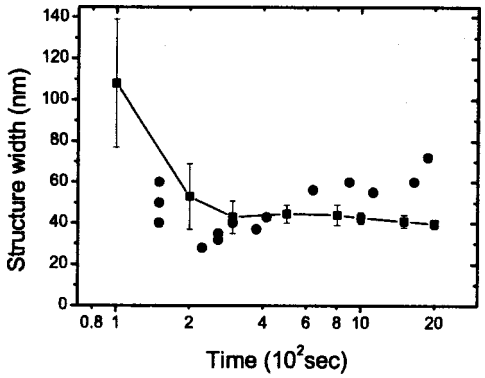

FIG. 8. Structure width as a function of deposition duration. Line: simulations. Circles: experimental data. The slow increase in structure width at long deposition times is not reproduced, whereas the rapid decrease at short deposition times is.

C. Deposition duration

Finally, we investigate the dependence on deposition duration, which we also compare to the experimental data.[9] As shown in Fig. 8, the width of the experimental structures is large with a large uncertainty for very short depositions, after which the structures become rapidly narrower. At longer deposition times, the width of the structures increases slowly. Our simulations reproduce the initial increased width of the structures at least qualitatively. Simulation runs using a larger sample at short deposition times show that the increased scatter in structure widths is not a statistical fluke, but rather a consequence of increased scatter in the outcomes.

At longer deposition times, our simulations fail to reproduce the slow increase in structure width. We find three possible explanations for this. One reason is that the barrier to diffusion thrown up by the pollutants is too absolute in our simulations. By this we mean that in real, two-dimensional depositions, the presence of a pollutant does not mean an absolute barrier: an atom *could* diffuse around it. In our one-dimensional simulated surface, there is no way around a pollutant at all. Second, there is also the possibility of thermal or other drifts of the substrate relative to the standing wave. The drift that would need to occur is something of the order of 10 nm over a mirror-to-line distance of around 2 mm. This means a relative length change of around 5×10^{-6}. If we attribute this to a thermal expansion of the Si substrate, the temperature drift needed is around 2 K. Note that structure width dependence on thermal drift is something different altogether from dependence on absolute temperature. A third effect could be that diffusion of the pollutant species is not completely absent, but just much slower. We deem this relatively unlikely, as it would require a very specific activation energy of pollutant diffusion.

V. ES-BARRIER LIMITED SURFACE DIFFUSION

As in the previous section, we begin our investigation of ES-barrier effects by looking at the structures predicted. Figure 9 displays four of the simulated structures for two different values of the ES barrier; $E_{ES} = 0.2$ eV at the top, and $E_{ES} = 0.09$ eV at the bottom. The biggest difference between

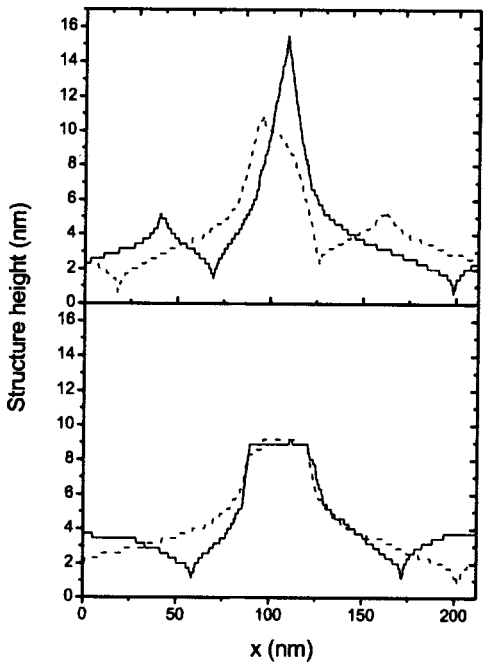

FIG. 9. Simulated structures with Ehrlich–Schwoebel barrier. Top: two simulation runs with identical initial conditions; $E_{ES}=0.2$ eV. Bottom: same, for $E_{ES}=0.09$ eV. Note the increased surface roughness of the structures at high ES barrier.

the two is the marked increase in surface roughness at higher E_{ES}. This is an expected effect. As the ES barrier increases an atom's residence time on a terrace, islanding will occur on smaller terraces, leading to increased roughening. However, experimental investigations, using a scanning electron microscope (SEM),[22] show no roughness on that scale. This leads us to discount the possibility of a very high ES barrier.

The next step is to determine the absolute value of the ES barrier. The simulated structure widths at various values of E_{ES} are shown in Fig. 10. The FWHM of the structures was determined as in Sec. IV. At low E_{ES}, the structures are very broad, and they become narrower with increasing E_{ES} until a value of around 100 meV. At higher values of E_{ES}, the structures no longer become much narrower, but the spread in their FHWM increases dramatically. This is a side effect of the increased surface roughness at high E_{ES}. Restricting ourselves to modest values of the ES barrier, we find the best agreement with experiment at a value of $E_{ES}=0.09$ eV. We will use this value in all following simulations.

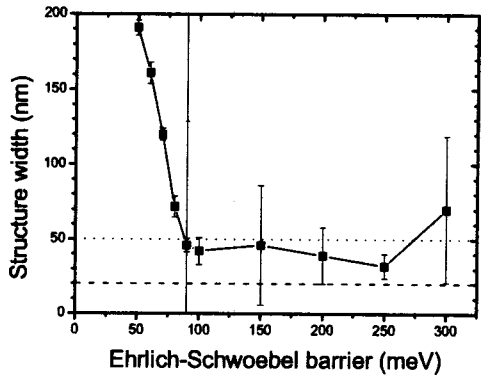

FIG. 10. Simulated structure width as function of E_{ES}. Dashed line: atomic flux width. Dotted line: experimental structure width. The large spread in outcomes at high E_{ES} is due to increased surface roughening for a high ES barrier, as seen in Fig. 9. Vertical line indicates model value.

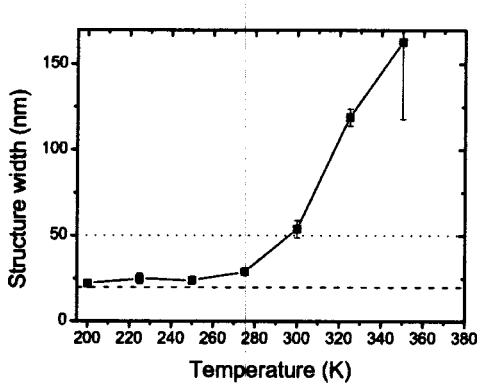

FIG. 11. Temperature dependence of structure widths in the ES-barrier model. Symbols: simulation results. Dashed line: atomic flux width. Dotted line: experimental structure width.

We now proceed to investigate the temperature dependence of the structures' width. Figure 11 shows the FWHM of the simulated structures as a function of temperature. The dependence of structure width on structure height is dramatic. At low temperatures, the ES barrier effectively appears to block nearly all diffusion. The resulting structures have widths similar to the width of the atom flux distribution. At higher temperatures, the width of the structures increases dramatically. This is in clear disagreement with the experimental findings of Anderson *et al.*[9] We believe that this is natural, as crossing the ES barrier is a thermally activated process. We conclude that, although an ES barrier very probably does exist for Cr, its effect is not such that it can explain the experimental data.

VI. CONCLUSIONS

We have modeled structure broadening by atomic diffusion in atom lithography. In our models, we have assumed that atomic diffusion occurs as a thermally activated process that is frustrated by some kind of barrier. We explore two different possible causes for this barrier. One mechanism is that pollutant adatoms from the vacuum background limit surface diffusion by posing a physical barrier. The alternative is that surface diffusion is limited by an ES barrier that is inherent in surface diffusion. We have performed kinetic Monte Carlo simulations of both limiting mechanisms.

The results of the pollutant-based simulation match the experimental results[9] very well. The barrier imposed by the pollutant species effectively suppresses the temperature dependence of the structure broadening. The only incongruence between our model and the experimental results is in the deposition time dependence of the structure widths. At longer deposition times, our model fails to predict the observed increase in structure broadening. This could be due to the one-dimensional nature of our simulations or to experimental drifts. A third possibility is that it is due to one of the

many possible diffusion processes we have neglected. The ES barrier utterly fails to reproduce the experimental lack of temperature dependence, and hence, we believe that it is not the dominant factor in surface diffusion of Cr.

The veracity of the claims we make here would be interesting to test experimentally. This would not be very difficult as all one has to do is to introduce a controlled leak in the deposition vacuum. Furthermore, the pollutant barrier might be exploited to tune structure widths in atom lithography. The diffusion model could be further refined by the inclusion of several slower diffusion processes, such as, for instance, step edge detachment and pollutant adatom diffusion.

ACKNOWLEDGMENTS

This work is financially supported by the Dutch Foundation for Fundamental Research on Matter (FOM). The authors wish to thank M. K. Oberthaler and D. Jürgens for useful discussions.

[1] H. Metcalf and P. van der Straten, *Laser Cooling and Trapping* (Springer, New York, 1999).
[2] D. Meschede and H. Metcalf, J. Phys. D **36**, R17 (2003).
[3] Th. Schulze, T. Müther, D. Jürgens, B. Brezger, M. K. Oberthaler, T. Pfau, and J. Mlynek, Appl. Phys. Lett. **78**, 1781 (2001).
[4] R. E. Behringer, V. Natarajan, and G. Timp, Appl. Phys. Lett. **68**, 1034 (1996).
[5] G. Timp, R. E. Behringer, D. M. Tennant, J. E. Cunningham, M. Prentiss, and K. K. Berggren, Phys. Rev. Lett. **69**, 1636 (1992).
[6] J. J. McClelland, R. E. Scholten, E. C. Palm, and R. J. Celotta, Science **262**, 877 (1993).
[7] R. W. McGowan, D. M. Giltner, and S. A. Lee, Opt. Lett. **20**, 2535 (1995).
[8] E. te Sligte, R. C. M. Bosch, B. Smeets, P. van der Straten, H. C. W. Beijerinck, and K. A. H. van Leeuwen, Proc. Natl. Acad. Sci. U.S.A. **99**, 6509 (2002).
[9] W. R. Anderson, C. C. Bradley, J. J. McClelland, and R. J. Celotta, Phys. Rev. A **59**, 2476 (1999).
[10] R. E. Behringer, V. Natarajan, and G. Timp, Appl. Surf. Sci. **104/105**, 291 (1996).
[11] E. Jurdík, Th. Rasing, H. van Kempen, C. C. Bradley, and J. J. McClelland, Phys. Rev. B **60**, 1543 (1999).
[12] R. M. Bradley, A. Eschmann, and S. A. Lee, J. Appl. Phys. **88**, 3316 (2000).
[13] A. Pimpinelli and J. Villain, *Physics of Crystal Growth* (Cambridge University Press, 1998).
[14] H. Brune, J. Wintterlin, R. J. Behm, and G. Ertl, Phys. Rev. Lett. **68**, 624 (1992).
[15] R. X. Ynzunza, R. Denecke, F. J. Palomares, J. Morais, E. D. Tober, Z. Wang, F. J. García de Abajo, J. Liesegang, Z. Hussain, M. A. van Hove, and C. S. Fadley, Surf. Sci. **459**, 69 (2000).
[16] A. C. Schindler, Ph.D. thesis, Gerhard-Mercator-Universität, Duisburg (1999).
[17] G. Gewinner, J. C. Peruchetti, A. Jaegle, and A. Kalt, Surf. Sci. **78**, 439 (1978).
[18] J. E. Simpkins and P. Mioduszewski, J. Vac. Sci. Technol. **20**, 1321 (1982).
[19] J. G. Amar and F. Family, Thin Solid Films **272**, 208 (1996).
[20] R. Stumpf and M. Scheffler, Phys. Rev. Lett. **72**, 254 (1993).
[21] S. J. Liu, H. Huang, and C. H. Woo, Appl. Phys. Lett. **80**, 3295 (2002); M. G. Lagally and Z. Zhang, Nature (London) **417**, 907 (2002).
[22] J. J. McClelland, R. Gupta, Z. J. Jabbour, and R. J. Celotta, Aust. J. Phys. **49**, 555 (1996).